

EVS29 Symposium
Montréal, Québec, Canada, June 19-29, 2016

A Mathematical and FEM Design of Novel Axial Field Switched Reluctance Motor for Electrical Vehicle (EV) Application

Nikunj R Patel¹, Varsha A Shah¹, Makarand M Lokhande²

¹*Department of Electrical Engineering, SV National Institute of Technology, Surat, nikunj80_patel@yahoo.com*

²*Department of Electrical Engineering, Visvesvaraya National Institute of Technology, Nagpur*

Abstract

Switch reluctance (SR) motors attract attention as a motor that does not use permanent magnet material. So it is a strong candidate for electrical vehicle (EV) application. In EV application axial flux machines are preferred over radial flux machines due to high power density. In this Article novel axial field switched reluctance motor (AFSRM) design is presented which intend to improve the output torque by single flux path distribution in C- core stator. Unlike conventional radial field SRMs, the windings of the C-core stator can be individually wound without complex winding equipment. This topology has an 8/6 pole dual air gap single rotor and single C-core stator configuration without overlapping winding arrangement. Computer Aided Design (CAD) is used to calculate the phase inductance and average torque for a novel AFSRM topology. The two and three-dimensional Finite element (FE) analyses is carried out to validate obtained CAD results.

Keywords: motor design, EV (electric vehicle), brushless motor, switching reluctance motor, wheel hub motor

1 Introduction

Transport activity, a key component for economic development and human welfare, is increasing around the world. Currently transportation system totally relies on fossil fuel resources that supplies 95% of the total energy used by world transport. But limited quantities of conventional energy sources like petroleum on earth and also the ever arising pollution disasters by these sources have propelled the search for alternate energy driven vehicles. Electric vehicles and hybrid vehicles has emerged as the best possible solution to tackle all the aforementioned issues. Additional energy requirements to charge the batteries has to be taken care without incorporating newer generation plants by either energy conservation or energy generation from non-conventional sources to make it zero pollution electric vehicle. The motor drive used for propulsion plays a significant role for maximizing the efficiency of EV and improving its performance. In recent years permanent magnet (PM) motors, induction motors and switched reluctance motors (SRM) has been used in motor drives of electrical vehicle for propulsion. Permanent magnet (PM) motors which offers high torque density and efficiency has the disadvantage of thermal problem which arises due to eddy currents. Also the employment of rare-earth magnetic materials which are expensive due to the monopoly of certain countries in their availability is another economical drawback. This has drawn considerable interest in research on switched reluctance motor (SRM) because it does not use any permanent magnets. SRM becomes a suitable candidate in Electrical Vehicle (EV) and Hybrid Electrical Vehicle (HEV) propulsion which needs high torque and high speed [1-2]. SRM has advantages like simple and rugged construction high speed operation and high-fidelity against impact and vibration under off-load condition. The main problems with the SRMs are noise and high torque ripple. However, these problems are being solved by development of the power electronics devices and their controls. It is difficult to output high torque because of the absence of permanent

magnet. Hence it is difficult to avoid a high current density and the motor mass becomes large due to increase in the torque. Based on field distribution SRM can be classified in to two, Radial field SRM and Axial Field SRM. Various radial field constructions of SRM are available in literature [3-8]. The axial magnetic field disk type SR motors is different from the traditional radial magnetic field SR machines, whose rotor core is laminated into disk shape. Because of the special structure, the axial length of this kind of motor can be reduced compared to the radial field motor. Due to small magnetic length, axial field motor offers high torque. Various topologies of axial flux SRM (AFSRM) have been reported in the literature [9-17]. In this paper a novel C-core axial field 8/6 SRM motor is proposed.

2 Novel axial field switch reluctance motor

AFSRM is consists of C-core stator with excitation winding on individual C-core and a winding less rotor. Rotor conductors are not required because the torque is produced by the tendency of the rotor to obtain minimum reluctance position. The performance analysis of SRM requires the dimensions for stator and rotor laminations, winding details, pole numbers, and pole arcs.

C-core axial field technique is novel structure due to its merits,

- (1) Separate C-core stator offers more space for winding and good thermal dissipation.
- (2) Higher power density and torque.
- (3) Single and isolated C-core offered easy maintenance.
- (4) Due to larger space and individual winding on individual C-core, magnetic losses are reduced and machine efficiency will increase.

In this paper the detailed design is carried out to arrive at the dimensions of the AFSRM. Initially, design is carried out using conventional method. The paper is divided into six sections. Section 3 summarizes basic electric vehicle dynamics and gives drive specifications; based on which AFSRM parameters are assumed. The mathematical modeling is prepared and torque equation is derived in section 4. The obtained CAD results and dimensions are validated using 2D and 3D FE analysis in section 5. The paper concludes with obtained results and advantages of proposed method in section 6.

3 Vehicle dynamics and sizing of AFSRM

Based on vehicle dynamic equations given below torque requirements have been derived for various driving conditions according to Indian driving cycle. Figure 1 gives a basic vehicle dynamic model [19].

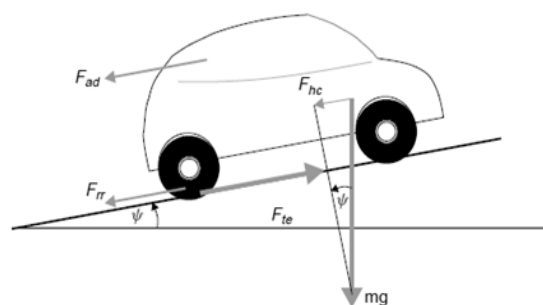


Figure 1: Vehicle dynamic models

$$\text{Tractive effort} = F_{te} = \frac{T_m}{r} \quad (1)$$

$$\text{Rolling Friction} = F_{rr} = \mu mg \cos \psi \quad (2)$$

$$\text{Air Drag} = F_{ad} = \frac{1}{2} v^2 \rho A C_d \quad (3)$$

$$\text{Angular acceleration, } a = \frac{dv}{dt} \quad (4)$$

$$\omega_m = \frac{v}{r} \quad (5)$$

$$F_{te} = F_{rr} + F_{ad} + mgsin\psi + ma + J / r^2 a \quad (6)$$

Where

T_m : Motor torque, r : Wheel radius, μ : Coefficient of rolling friction, ω_m : speed of motor C_d : Drag coefficient, ρ : Density of air, A : Frontal surface area, v : Velocity, g : Gravitational force, ψ : Inclination angle, m : mass of vehicle. Equation (6) is giving an idea about the torque and speed requirement of vehicle. By applying this equation for given data in Table I required torque is found out to be 24.6 Nm for flat surface.

Table I: Electrical vehicle parameter

	Rating
Mass of vehicle + 1 rider	186 kg
Inertia	Take into account by increasing mass by 5%
Frontal area	0.6 m ²
Inclination	0 deg.
Wheel radius	0.21 m
Drag coefficient	0.75
Coefficient of rolling friction	0.0007
Acceleration	0 to 45 kmph in 20 seconds

4 Design of axial flux switch reluctance motor

The design procedure of AFSRM is as follows. In this machine magnetic field is along and current is perpendicular to shaft. So it is comes under the axial field machine. The design specifications for the SRM comprise of the required power output (P_{hp}) in h.p., speed (N) in rpm, allowable peak phase current (I) in Amps, and available ac supply voltage (V_{ac}) in volts for the system. Knowing the speed and power output will automatically fix the torque to be developed by the machine as (7) [9].

$$T_{req} = \frac{P_{hp} * 745.6}{2\pi \left(\frac{N}{60}\right)} = \frac{P_{kw}}{2\pi \left(\frac{N}{60}\right)} N.m \quad (7)$$

Where P_{kw} is the power output in watts. In this paper 600 rpm is considered for design which produce 27.4 Nm torque.. Here rated speed is responsible for power rating of motor. Outer diameter of motor is assumed 250mm. The number of rotor and stator poles are finalized by the help of feasible triangle method as shown in figure 2. Once geometry parameters are finalised then select sheet steel material by comparing magnetic characteristics of different materials. Determine aligned and unaligned inductance of machine using magnetic equivalent circuit. Using aligned and unaligned inductance and geometry parameters torque equation is derived. Finally CAD is prepared and satisfactory results were found. The assumed designed data are given in Table II.

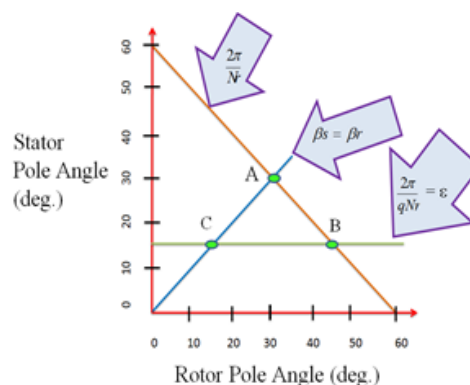


Figure 2: Feasible triangle for 8/6 AFSRM

Table II: 8/6 Dimensions AFSRM

Parameters	Symbol	Values
Number of stator/rotor poles	P_s/P_r	8/6
Number of phases	q	4
Outer diameter of rotor (mm)	D_{or}	250
Inner diameter of rotor (mm)	D_{ir}	156
Axial Length of motor	L	140
Air-gap length (single side) (mm)	l_g	0.5
Stator pole pitch (deg.)	β_{ps}	45
Stator pole arc (deg.)	β_s	22
Stator C-core thickness (mm)	t_s	47
Rotor pole pitch (deg)	β_{pr}	60
Rotor pole arc (deg)	β_r	23
Rotor pole length (mm)	l_{rp}	25
No. of turns/pole	N_p	115
Shaft Diameter (mm)	D_{sh}	60

4.1 Material selection

The different magnetic characteristics of different materials are shown in figure 3. It can be observed that, Sheet, cast, and silicon steel have good magnetic profile compared to other magnetic material. Among these, sheet steel material's B-H characteristic is used in the stator and rotor stamping. The "knee" point of the material characteristics is considered and it is usually a good design practice to limit the maximum flux density (B_{max}) (in Tesla) in any part of the machine to this value. It can be observed that the maximum flux density (B_{max}) will be at the stator poles and therefore while designing the machine, the stator pole can be assumed to be operating at a flux density equal to the knee value obtained from the B-H characteristics. The stator pole flux density (B_{ms}) is assumed to be equal to $B_{max} = 1.58T$ base on this consideration the rest of the machine is designed.

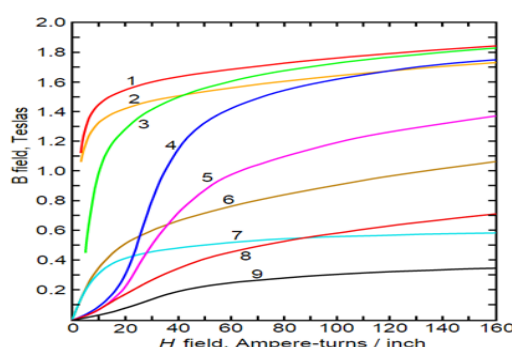


Figure 3: Magnetization curves of 9 ferromagnetic materials, showing saturation. 1. Sheet steel, 2.Silicon steel, 3.Cast steel, 4.Tungsten steel, 5.Magnet steel, 6.Cast iron, 7.Nickel, 8.Cobalt, 9.Magnetite

4.2 Magnetic equivalent circuit

A magnetic equivalent circuit (MEC) is developed for determining the phase inductance of axial field switch reluctance motor (AFSRM). Figure 4 shows the magnetic equivalent circuit of AFSRM for aligned and unaligned condition with 3D-FE analysis model for a single stator core. Different parts of an electrical machine namely rotor, stator and air gap is schematically represented. The reluctance of the stator pole, rotor pole and air-gap flux path are denoted as R_s , R_r , R_g respectively. From figure 4(b) it can be observed that in unaligned condition aligned flux (\emptyset) divides into two parallel paths.

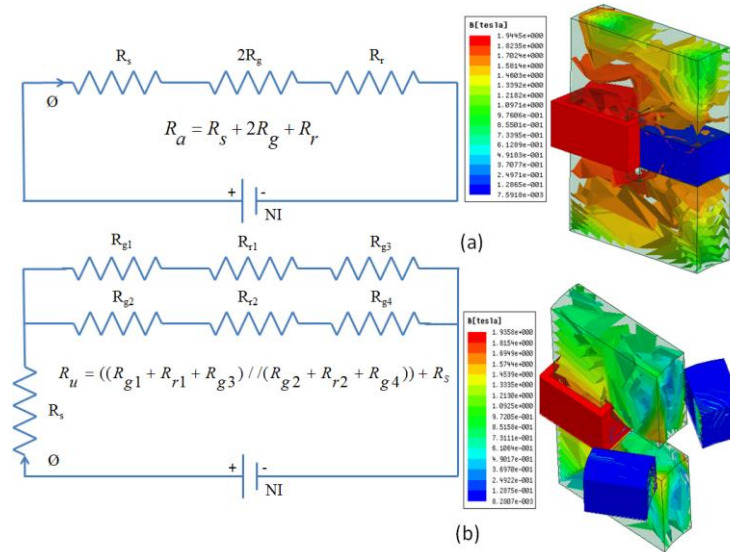


Figure 4: Magnetic equivalent circuit with single core 3D FE model for (a) aligned position, (b) unaligned position

The aligned reluctance is (R_a)

$$R_a = R_s + 2R_g + R_r \tag{8}$$

Similarly by the help of figure 4(b) it is possible to find unaligned reluctance (R_u).

$$R_u = ((R_{g1} + R_{r1} + R_{g3}) || (R_{g2} + R_{r2} + R_{g4})) + R_s \tag{9}$$

Where,

$$R = \frac{Hl}{BA} \tag{10}$$

Here l is the total length of set-up flux path. A is a particular correctional area where flux is set-up. B represents the flux density at concern part. H is a magnetic flux intensity which depends on the ampere turns (NI). Based on the geometrical parameter of the motor NI and torque (T_m) offered by motor can be calculated.

4.3 Mathematical design

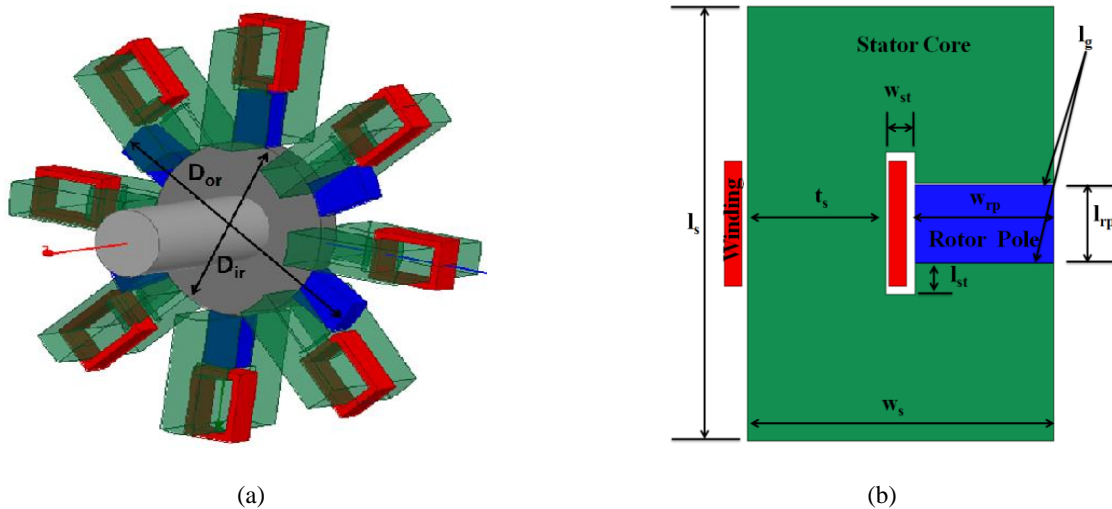


Figure 5: (a) 3D view of the motor (b) 2-D cross-sectional view of single stator core

Figure 5 (a) shows the complete 3D view of the proposed AFSRM. It consists of single inner-rotor disc with six poles and outer-stator with eight C-core arrangement. Stator and rotor are made by sheet steel. The

winding is provided on individual stator pole. Two coils are connected in series to form a phase. The number of working pole pair per phase is 2 for 8/6 pole AFSRM. In this paper primary focus is on the popular combination of 8 stator and 6 rotor poles. This machine offers lesser torque ripple than the other common combination of 6/4. Overall outer diameter, number of rotor and stator poles and axial length of the machine are considered constant. Rotor pole angle (β_r) and stator pole angle (β_s) are selected based on following conditions.

$$\text{Condition 1: } \beta_r \geq \beta_s, \quad \text{Condition 2: step angle } \varepsilon = \frac{2\pi}{q \cdot N_r} < \beta_s, \quad \text{Condition 3: } \frac{2\pi}{N_r} - \beta_r > \beta_s$$

The stator pole arc must be smaller or equal to rotor pole arc for reduce the torque ripple. To achieve the self-starting required step angle (ε) must be smaller than stator pole arc. Condition 3 is useful to obtain good relation of aligned to unaligned inductance, which is responsible for torque production of AFSRM. It is required to calculate the flux density at stator, rotor and air-gap. Figure 4(a) shows the stator flux (Φ_s) is setup in entire single stator C-core for fully aligned condition. The area of stator pole is same as the area of effective air gap. Overlap area (A_o) between the rotor pole and stator pole is same as the area of A_s .

$$B_{mr} \times A_r = B_{ms} \times A_s = B_{mg} \times A_g \quad (11)$$

Air gap flux density (B_{mg}), rotor flux density (B_{mr}) and stator flux density (B_{ms}) can be calculated from (11). The magnetic field intensity of stator H_s , rotor H_r and air gap H_g can be find out by given B-H graph. The reluctance of the stator core (R_s), rotor pole (R_r), and air gap (R_g) can be consider as a series circuit as shown in figure 4(a) for aligned condition and figure 4(b) for un-aligned condition. The lumped parameter $R_L = R_a$ is obtained as shown in (8). The reluctance (R) depends on correctional area (A), flux density (B), mean length of flux set-up (l), and magnetic flux intensity as shown in equation (10). As show in Figure 5, the diameter of various magnetic parts along the axial length (L) of the motor is equal to the stator length (l_s). The rotor pole length (l_{rp}) is considered 25mm and air gap length (l_g) = 0.5 mm for single side. Rotor pole width is denoted by (w_{rp}). The width (w_{rp}) depends on difference of rotor outer diameter (D_{or}) and rotor inner diameter (D_{ir}). For uniform distribution of flux stator core thickness is equal to rotor pole width $t_s = w_{rp}$. For the aligned condition length (l) of the set flux path is given by

$$l = l_s + 2l_{st} + 2w_s - 2t_s \quad (12)$$

The magnetic circuit equation is written as

$$NI = 2(H_g l_g) + (H_s l_s) + (H_r l_r) \quad (13)$$

From (13) total ampere turn NI required per phase for the machine to operate at full load by considering maximum flux density of material is estimated. The peak current I is assumed initially for calculating per phase conductors required. The equiflux tubes have been plot for calculating the unaligned inductance [9]. Here calculation is carried out for eight tubes. The torque expression for AFSRM is derived using sizing equation. A basic inductance and torque equation is applicable for SRM [18]

$$T_{avg} = \frac{1}{2} I^2 \frac{dL}{d\theta} \quad (14)$$

By using (14) Torque equation for the single C-core is derived as presented in this paper where aligned inductance and unaligned inductance are L_a and L_u .

$$T_{avg} = \frac{(I^2 \times L_a \times K \times q \times P_r)}{4 \times \pi} \quad (15)$$

Where,

$$K = 1 - \frac{L_u}{L_a} \quad (16)$$

Where k depends on the ratio of unaligned and aligned inductance, where q is number of phases. If applied to different computation planes for calculating, it gives effective result [19]. By using sizing parameters in Table II and mathematical equations the results obtained are given in Table III.

Table –III: Analytical result of AFSRM

Topology	L_a	L_u	T_{avg}
AFSRM	12.03mH	3.05mH	27.4Nm

5 Finite element modelling and simulation of AFSRM

A C-core AFSRM model is built using 2D and 3D finite element simulator software. The main dimension of stator and rotor are decided from mathematical sizing equation. Single core is considered for electromagnetic analysis, where the mesh is implemented for 2D and 3D model for getting an accurate result. Figure 6(a) illustrates the FE flux-plot at rated current 40A. As the rotor pole moves more toward the full alignment position, the saturation level increases and covers more regions. Figure 6(b) shows flux linkage as function of magneto-motive force for single stoke range, from unaligned to aligned position of the rotor. It can be observed in the graph that the curve of the aligned position starts to be saturated at 15A. Here 3D FEA-based motion model is employed at discrete speeds in order to investigate the dynamic performance of motor over the full-speed range operation. A 3-D FEA is extremely time-consuming for entire speed region. But in 2D analysis depth of the model does not come in to the calculation effectively. Due to this problem 3D part analysis is performed.

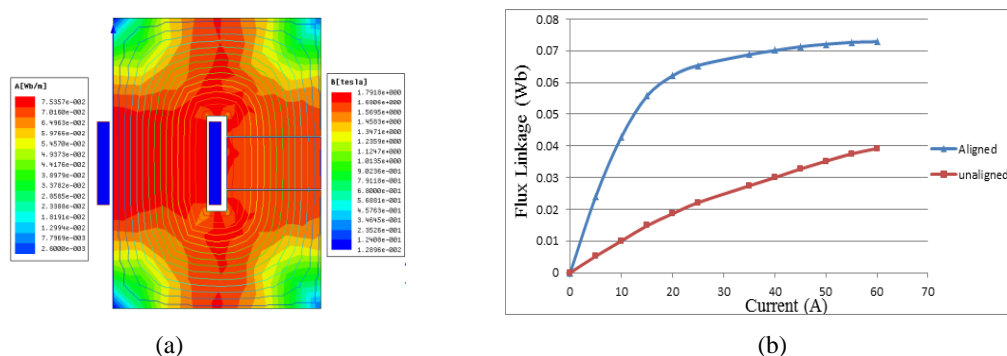


Figure 6: 2D FE analysis of AFSRM (a) Magnetic flux density plot, (b) Magnetic saturation characteristic

It should be noted that the mathematical calculations, results and analyses are presented for a single-coil and single phase computation. This is reasonable due to the complete separation between all C-core magnetic circuits. The mutual inductance between coils is neglected due to sufficient spacing. Figure 7 shows torque profile at different position for single coil excitation. Two coils come under one phase. Figure 8 represent the torque profile for one phase/two coils excitation. Table IV gives a comparison between the analytical and FEM results. No major difference in analytical and graphical results.

Table: IV Comparison of CAD and FEM results

No. of turns	Current	CAD	FEM	FEM
(Number)	Ampere(A)	Torque in Nm For single core	Torque in Nm For single core	Torque in Nm For one phase
115	40	13.7	12.49	25.5

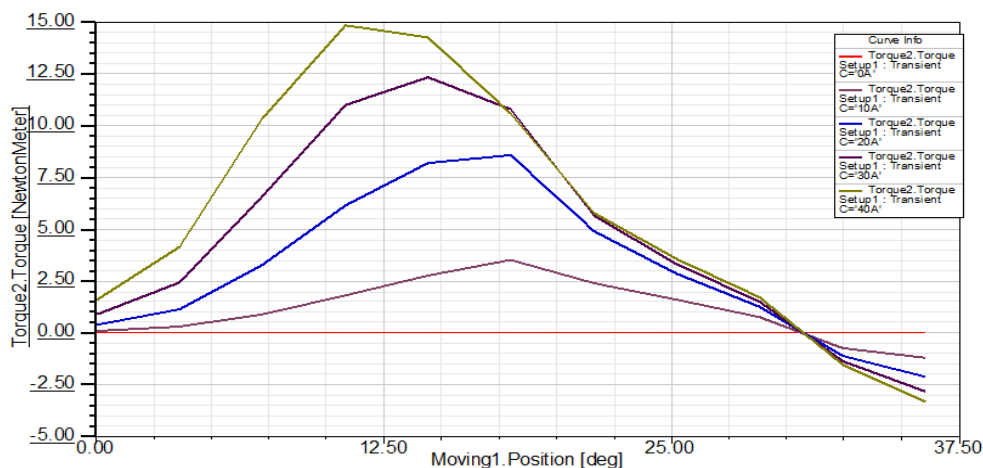


Figure 7: Torque profile of single coil excitation

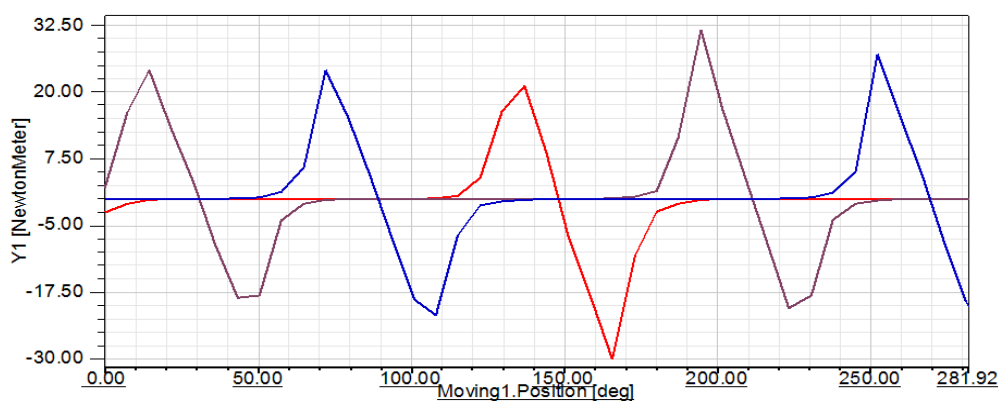


Figure 8: Torque profile under one phase excitation

6 Conclusion

In this paper a novel axial flux C-core switched reluctance motor is proposed for electrical vehicle application. In this topology shorter and single flux path offers good torque. It reduces leakage flux and end winding volume. This design offers easy and less skilled winding structure. The relation that exist between the physical dimensions and reluctances as well as torque where exploited for quickly arriving at the desired motor design. A 2D and 3D model are developed for performance evaluation of machine. A mathematical design is prepared for the sizing of this machine and validating the same with FEA tool.

References

- [1] Li Weili, Sheng Man, Huo Fei "Optimal design and Finite Element Analysis of Switched Reluctance Motor for Electric Vehicles" *IEEE Vehicle power and Propulsion Conference (VPPC), 2008, China J. Clerk Maxwell, A Treatise on Electricity and Magnetism, 3rd ed., vol. 2. Oxford: Clarendon, pp.68–73, 2011.*
- [2] K. Watanabe, S. Aida, A. Komatsuzaki, I. Miki "Driving Force Characteristics of 40kW Switched Reluctance Motor for Electric Vehicle" *International Conference of Electrical Machines and Systems, Elissa, pp. 1894-1898K, 2007.*
- [3] Zhan Qionghua, Wang Shuanghong, Ma Zhiyan, Guo Wei, Qiu Yihui "Design of a 50kW Switched Reluctance Machine for HEV Propulsion System" *Vehicular Technology Conference. VTC 2003-Fall. IEEE 58th, Vol.5 pp.3207-3211, 2003.*
- [4] S. Smaka, S. Masic, M. Cosovic, I. Salihbegovic "Switched Reluctance Machines for Hybrid Electric Vehicles" *XIX International Conference on Electrical Machines (ICEM), Rome, 2010.*
- [5] R. Vandana, K. Saikrishana "A new excitation scheme for polyphase segmented switched reluctance

- motor” *Energy Conversion Congress and Exposition (ECCE), IEEE*, pp.2667-2671, 2010.
- [6] Wen Ding, Yanfang Hu, Qiji Ze, Xing Liu, Yunpeng Liu “A Novel Modular E-Core Stators and Segmental Rotors Switched Reluctance Machine for Electric Vehicles”, *Ninth International Conference on Ecological Vehicles and Renewable Energies (EVER), IEEE*, pp.1 – 8, 2014.
- [7] Shang-Hsun Mao and Mi-Ching Tsai, “A Novel Switched Reluctance Motor With C-Core Stators”, *IEEE Transactions On Magnetics, Vol. 41, NO. 12*, pp.4413-4420, Dec- 2005.
- [8] Wang Yaling, Xu Yanliang, Wang Yufang, Zhang Yun, “Outer-Rotor Switched Reluctance Motor and its Control System Used in Electric Vehicles”, *Electrical Machines and Systems (ICEMS), IEEE International Conference*, pp.1 - 4, 2011.
- [9] R. Krishnan, M. Abouzeid, and X. Mang, “A design procedure for axial field switched reluctance motors,” in *Proc. Ind. Appl. Soc. Annu. Meet*, pp. 241–246, 1990.
- [10] A. Labak and N. C. Kar, “A novel five-phase pancake shaped switched reluctance motor for hybrid electric vehicles,” in *Proc. Int. Conf. Veh. Power Propulsion*, pp. 494–499, 2009.
- [11] A. Labak and N. C. Kar, “Development and analysis of a five-phase pancake shaped switched reluctance motor,” in *Proc. Int. Conf. Elect. Mach.*, pp.1–6, 2010.
- [12] H. Arihara and K. Akatsu, “A basic property of axial type switched reluctance motor,” in *Proc. Int. Conf. Elect. Mach. Syst.*, pp.1687–1690, 2010.
- [13] H. Arihara and K. Akatsu, “Characteristics of axial type switched reluctance motor,” in *Proc. Energy Convers. Congr. Expo.* pp. 3582– 3589, 2011.
- [14] H. C. Lovatt, E. Darrell, L. Cahill, D. H. Huynh, A. stumpf, A. Kulkarni, A. Kapoor, M. Ektesabi, H. Mazumder, T. Dittmar, and G. White, “Design procedure for low cost, low mass, direct drive in-wheel motor drive trains for electric and hybrid vehicles,” in *Proc. Annu. Conf. Ind. Electron. Soc.*, pp. 4558–4562, 2011.
- [15] P. Bolognesi, “Design and manufacturing of an unconventional variable reluctance machine,” in *Proc. IET Power Electron., Mach. Drives*, 2008.
- [16] L. P. Tessier, J. P. Doyle, and J. L. Weber, “Axial flux switched reluctance motor and methods of manufacture,” *U.S. Patent 0295389*, Nov. 25, 2010.
- [17] Y. C. Lee and C. C. Yang, “Multi-unit modular stackable switched reluctance motor system with parallel excited low reluctance circumferential magnetic flux loops for high torque density generation” *U.S. Patent 0001502*, Jan., 2012.
- [18] T.J.E. Miller, *Switched Reluctance Motors and their Control*, London, U.K.: CRC Press, 1993.
- [19] R. Madhavan and B. G. Fernandes, “A novel axial flux segmented SRM for electric vehicle application,” in *Proc. Int. Conf. Elect. Mach*, 2010.

Authors

Nikunj Patel was born in Gujarat, India. He received the B.E Degree in Electrical Engineering from South Gujarat University, Surat, India in 2004, and the M.Tech. Degree in Electrical Engineering from NIRMA University, Gujarat, India in 2009. He is pursuing his PhD in the Department of Electrical Engineering of Sardar Vallabhbhai National Institute of Technology, Gujarat, India. He has been working as an Assistant Professor in the Department of Electrical Engineering of SSASIT Surat, India from 2009. His research interests are in machine modelling, analysis and design for Electric Vehicles applications.



Varsha A Shah was born in Surat, India. She received the B.E Degree in Electrical Engineering from Maharaja Sayajirao University, Gujarat, India in 1986, the M.E. Degree in Electrical Engineering from Veer Narmad South Gujarat University, Gujarat, India in 1990 and the Ph.D. Degree in Electrical Engineering from Sardar Vallabhbhai National Institute of Technology, Gujarat, India in 2013. She has been working as an Associate Professor in the Department of Electrical Engineering of Sardar Vallabhbhai National Institute of Technology, Gujarat, India from 1987. Her research activity is related to hybrid electric vehicles, smart grid and power quality issues.



Makarand M Lokhande was born in Nagpur, India. He received the B.E Degree in Electrical Engineering from Nagpur University, Maharashtra, India in 2001, the M.E. Degree in Electrical Engineering from the University of Pune, Maharashtra, India in 2003 and the Ph.D. Degree in Electrical Engineering from Indian Institute of Technology Bombay, Maharashtra, India in 2010. He has been working as an Assistant Professor in the Department of Electrical Engineering of Visvesvaraya National Institute of Technology, Maharashtra, India from 2015. Prior to that he was also associated with Sardar Vallabhbhai National Institute of Technology Gujarat, India and Pandit Deendayal Petroleum University Gujarat, India. His research activity is related to hybrid electric vehicles and Renewable Energy and Management.

